Biochimica et Biophysica Acta 1860 (2016) 1728–1738

Contents lists available at ScienceDirect

Biochimica et Biophysica Acta

journal homepage: www.elsevier.com/locate/bbagen

Towards personalized diagnostics via longitudinal study of the human plasma *N*-glycome☆

René Hennig [a,b], Samanta Cajic [a], Matthias Borowiak [b], Marcus Hoffmann [a], Robert Kottler [a], Udo Reichl [a,c], Erdmann Rapp [a,b,*]

[a] Max Planck Institute for Dynamics of Complex Technical Systems, Sandtorstrasse 1, 39106 Magdeburg, Germany
[b] glyXera GmbH, Leipziger Straße 44, 39120 Magdeburg, Germany
[c] Otto-von-Guericke University, Chair of Bioprocess Engineering, Universitätsplatz 2, 39106 Magdeburg, Germany

ARTICLE INFO

Article history:
Received 13 February 2016
Received in revised form 24 March 2016
Accepted 25 March 2016
Available online 31 March 2016

Keywords:
Glycomics
N-glycosylation
xCGE-LIF
Long-term stability
Longitudinal study
Personalized diagnostics

ABSTRACT

Facilitated by substantial advances in analytical methods, plasma *N*-glycans have emerged as potential candidates for biomarkers. In the recent years, several investigations could link aberrant plasma *N*-glycosylation to numerous diseases. However, due to often limited specificity and sensitivity, only a very limited number of glycan biomarkers were approved by the authorities up to now. The inter-individual heterogeneity of the plasma *N*-glycomes might mask disease related changes in conventional large cross-sectional cohort studies, with a one-time sampling approach. But, a possible benefit of longitudinal sampling in biomarker discovery could be, that already small changes during disease progression are revealed, by monitoring the plasma *N*-glycome of individuals over time. To evaluate this, we collected blood plasma samples of five healthy donors over a time period of up to six years (min. 1.5 years). The plasma *N*-glycome was analyzed by xCGE-LIF, to investigate the intra-individual *N*-glycome variability over time. It is shown, that the plasma *N*-glycome of an individual is remarkably stable over a period of several years, and that observed small longitudinal changes are independent from seasons, but significantly correlated with lifestyle and environmental factors. Thus, the potential of future longitudinal biomarker discovery studies could be demonstrated, which is a further step towards personalized diagnostics. This article is part of a Special Issue entitled "Glycans in personalised medicine" Guest Editor: Professor Gordan Lauc.

1. Introduction

Already in 1900 Karl Landsteiner carried out a simple experiment. By mixing serum and red blood cells from six of his colleagues he observed agglutination. This observation he published 1901, postulating three different blood types A, B and C (later O), as the cause of blood agglutination [1]. Since his discovery, blood became the main diagnostic source for determining and monitoring the physiological and biochemical state of a patient. But, it took about 50 more years of research before carbohydrates were identified as serologically active fragments responsible for the different blood groups [2], and another couple of decades to develop respective glycoanalytical methods, that enabled first insights into the (blood)glycome [3–9]. This reveals the enormous challenges that had to be overcome to analyze complex carbohydrates and carbohydrate conjugates.

Still during the last decade substantial advances have been made in analytical methods and analysis software in proteomics, glycoproteomics and glycomics, enabling more in-depth analyses of the human blood plasma glycans and glycopeptides [6,8–18]. Especially, the development of high-throughput (HTP) *N*-glycan profiling methods in CE, MS and HPLC [4,6,10,19,20] facilitated enrollment of glycomics in blood biomarker discovery. By analyzing big cohorts, alterations in *N*-glycan profiles from blood plasma have been found to correlate with pathological states, such as diabetes type II [21], inflammation [22], liver cirrhosis/fibrosis and cancer [23–26], as well as in breast [27–29], pancreas [30,31], ovaries [32], prostate [33], stomach [34,35] and lung [36] cancer. Furthermore, in large scale population studies *N*-glycosylation appeared to be associated with gender and age [37–39], as well as with hormonal changes in pregnancy [39–41].

Despite all this tremendous work, monitoring of glycosylation alteration during disease progression is still difficult and especially the early disease diagnostics turned out to be even more challenging. Due to an often limited specificity of the found glycan biomarker, statements are often vague and the false positive rate can be high [42–44]. As a result only a very few biomarkers were approved by the authorities in the past [22,29,42]. Accordingly, the limited specificity of *N*-glycan

☆ This article is part of a Special Issue entitled "Glycans in personalised medicine" Guest Editor: Professor Gordan Lauc.

* Corresponding author at: Max Planck Institute for Dynamics of Complex Technical Systems, Sandtorstrasse 1, 39106 Magdeburg, Germany.
E-mail address: rapp@mpi-magdeburg.mpg.de (E. Rapp).

http://dx.doi.org/10.1016/j.bbagen.2016.03.035

biomarkers might be caused by the large biological variability between individuals in large scale studies. This was already described by Knežević et al. [45], focusing on variability and heritability of human plasma *N*-glycome in a population study of 1008 individuals. For all above-mentioned cross-sectional biomarker studies a single sample was taken at only one time point from hundreds of individuals, from healthy controls and patients suffering from the same disease. Subsequently, a correlation analysis of the disease with the overall plasma *N*-glycomes was performed, potentially impaired by variation of different individuals [21–23,35,42,44,46,47]. Thus, trends might have been attenuated by the differences between individuals.

This raises the questions: "Are disease caused changes really significant compared to the differences between individuals, and how representative is a sample taken from a person at only one time point, respectively, how stable is the *N*-glycome of a person over time?" Up to now, only Gornik et al. showed a short term stability of the individual human *N*-glycome, by taking a time series of seven samples over five days. Furthermore, they demonstrated that the differences between two *N*-glycome samples, taken with an interval of approximately one year, are small [48]. We here investigated for the first time, the long-term stability of the human plasma *N*-glycome of individuals, by monitoring five healthy donors over a time period of up to six years (min. 1.5 years), to evaluate the potential of *N*-glycans as biomarkers for personalized diagnostics. Thus, for this longitudinal study, plasma samples were taken in short intervals for one year, to evaluate seasonal variations, followed up by sampling in larger intervals, to evaluate the stability of the plasma *N*-glycome over years. Since gender, age and smoking are identified as influencing factors [45], only non-smoking male volunteers of the same age were included into the study, minimizing the impact of these parameters. To estimate the impact of lifestyle and environmental factors on the plasma *N*-glycome, parameters such as illness, allergy, sleep behavior, as well as food and alcohol consumption were carefully documented for each volunteer. The analysis of the plasma *N*-glycome was performed by multiplexed capillary gel electrophoreses with laser induced fluorescence detection (xCGE-LIF), also known as DNA-sequencer-adapted fluorophore-assisted-electrophoresis (DSA-FACE). In addition we are presenting here a refined annotation of *N*-glycan peaks for both, the native (sialylated) and the asialo (desialylated) human plasma *N*-glycome. This might help to better assess and compare published xCGE-LIF (native plasma) [5,6,10,35,41,49,50] and DSA-FACE (asialo plasma) [23,47,51–53] results.

2. Materials and methods

2.1. Materials and reagents

2-Picoline-borane (2-PB) (≥95%, 654213), acetic acid (AA) (for luminescence, 45725), acetonitril (ACN) (LC–MS Grade ≥ 99.5%, 34967), aminopyrene-1,3,6-trisulfonic acid (APTS) (for fluorescence, ≥96.0%, 09341), dimethylsulfoxide (DMSO) (for HPLC, ≥99.7%, 34869), IGEPAL CA-630 (IGEPAL) (for molecular biology, I8896), phosphate buffered saline (PBS) (10× concentrated, BioReagent, P5493-1L), Peptide *N*-glycosidase F (PNGase F) (BioReagent ≥95%, P7367) and triethylamine (TEA) (≥99.5%, 471283) were obtained from Sigma-Aldrich (Germany). Citric acid monohydrate (CA) (ACS grade for analysis, 1002440500) was obtained from Merck-Millipore (Germany), ethanol (EtOH) (≥99.8%, T868.3) from Carl Roth (Germany), sodium dodecyl sulfate (SDS) (≥99%, A2572) from AppliChem (Germany) and Bio-Gel P10 (BioGel) (150-4144) from Bio-Rad (Germany). For sample preparation 96 well polypropylene microplates (96-W plate) (651201) from Greiner Bio-One (Germany), 0.8 mL 96 well storage plates (96-W storage plate) (AB-0765) from Thermo Scientific (Germany) and AcroPrep™ 96-well GHP Filter Plates (FilterPlate) (5030) from Pall Corporation (Germany) were used. As described in detail by Hennig et al. [54] for xCGE-LIF analysis Hi-Di™ Formamide (HiDi) (4311320), POP-7™ Polymer (4363785), GeneScan™ 500 LIZ™ Size Standard (LIZ standard) (4322682), MicroAmp® Optical 384-Well Reaction Plate (384-W plate) (4309849), 384-Well plate septa (Septa) (4315934) and 16-capillary array (capillary array) (4315930) were obtained from Life Technologies (Germany). Deionized water with $R > 18.2\ M\Omega * cm^{-1}$ (MilliQ™ water) was produced by a Gradient A10 system from Merck-Millipore (Germany). Minivette® POCT (50 μL, K3 EDTA, 17.2113.050) and Safety-Lancet (20–100 μL, 85.1017) were obtained from Sarstedt (Germany). Frozen normal control plasma (VisuCon-F, FRNCP0105) was obtained from Stago BNL (Netherlands). Octeniderm® farblos (skin disinfectant) was obtained from Schülke & Mayr (Vienna). Exoglycosidases α(2-3) sialidase (Sialidase S, GK80020), α(2-3,6,8) sialidase (Sialidase A, GK80040), α(1-2,3,4,6) fucosidase (GKX-5006) and α(1-2,3,6) mannosidase (GKX-5010) were purchased from Prozyme (USA). Exoglycosidases β(1-4) galactosidase (P0730L) and β(1-2,3,4,6)-*N*-Acetylglucosaminidase (P0732L) were purchased from New England Biolabs GmbH (Germany). α(1-3,4) fucosidase (E-F134) was purchased from QA-Bio (USA).

2.2. Longitudinal sample collection

Plasma samples from healthy volunteers were obtained by a minimal invasive sampling technique, according to a standard protocol for dried blood spots [55]. Briefly, a fingertip was cleaned with skin disinfectant and pricked with a Safety-Lancet. First blood droplet was removed by a sterile wipe. Following drops were collected with an EDTA filled 50 μL Minivette® and transferred to a 0.5 mL tube. Blood plasma was separated by centrifugation at 1500 *g* for 10 min at 4 °C, transferred to new 0.5 mL tubes and frozen until analysis at −80 °C. To avoid additional freeze and thawing cycles, all samples were analyzed in November 2014 (storage time: two to five years — depending on the sampling time point), except the samples from 2015 of volunteer 5.

Samples were collected from five healthy volunteers (male, non-smoking, same age: all 28 years old in 2011) within the time course of one year: for three months at weekly intervals, followed by three months at biweekly and six months at monthly intervals. Additional samples were taken within the time span of six years. Several environmental factors were documented like illness, diet, allergy and alcohol consumption (data collected for the period two days before sampling).

2.3. N-glycan release and labeling

N-glycans were released from plasma proteins as described previously [6], with slight modifications. Briefly, for denaturation 2 μL of plasma samples was mixed with 4 μL of 2% SDS_{PBS} (w/v) (=2% SDS:98% PBS_{aq}) and incubated for 10 min at 60 °C. Subsequently, remaining SDS was neutralized by adding 4 μL 8% $IGEPAL_{PBS}$ (v/v) (=8% IGEPAL:92% PBS_{aq}). *N*-glycans were released from denatured and linearized plasma proteins for 3 h at 37 °C by addition of 0.5 units PNGase F in 1 μL PBS_{aq}. Labeling of released *N*-glycans was performed for 16 h at 37 °C by mixing 2 μL of *N*-glycan solution with 2 μL of 20 mM APTS in 3.6 M CA_{aq} and 2 μL 0.2 M 2-PB in DMSO. To stop the labeling reactions 100 μL of 80% ACN_{aq} (v/v) (=80% ACN:20% MilliQ water) was added and samples were mixed carefully.

2.4. Hydrophilic interaction chromatography based solid phase extraction (HILIC-SPE)

Post derivatization sample clean-up was performed by HILIC-SPE to remove free APTS, reducing agent and other impurities as published in [54]. Briefly, 200 μL of a 100 mg/mL BioGel suspension in MilliQ™ water/EtOH/ACN (70:20:10%, v/v) was applied to FilterPlate. Solvents were removed by application of vacuum using a vacuum manifold (Merck-Millipore, Germany). All wells were prewashed with 3 × 200 μL MilliQ™ water, followed by an equilibration with 3 × 200 μL 80% ACN_{aq}. APTS labeled samples were loaded onto wells containing BioGel

suspension and shaken at 500 rpm for 5 min on a Thermomixer (to improve glycan binding). For purification wells were subsequently washed using 5 × 200 μL 80% ACN_{aq} containing 100 mM TEA adjusted to pH 8.5 with AA, followed by washing 3 × 200 μL 80% ACN_{aq}. All washing steps were performed by addition of solutions, incubation for 2 min and removal of solvent by vacuum. For elution 1 × 100 μL (swelling of BioGel) and 2 × 200 μL MilliQ™ water were applied to each well followed by 5 min incubation at 500 rpm on the Thermomixer. The eluates were removed by vacuum and collected in a 96-W storage plate. The combined eluates were either analyzed immediately by xCGE-LIF or stored until analysis at −20 °C (for max. 48 h).

2.5. Sample measurement using xCGE-LIF

xCGE-LIF measurement was performed as published [6,10,54]. Briefly, 1 μL of *N*-glycan eluate was mixed with 1 μL LIZ standard (1:50 dilution in HiDi) and 9 μL HiDi. The mixture was transferred to a 384-W plate, sealed with a septum and centrifuged for 1 min at 200 g to avoid air bubbles at the bottom of the wells. The xCGE-LIF measurement was performed in a 3130xl Genetic Analyzer, equipped with a 50 cm capillary array, filled with POP-7™ polymer. The samples were electrokinetically injected and analyzed with a running voltage of 15 kV. Data was collected for 40 min.

2.6. Data analysis and structural characterization

Raw data files were converted to xml file format and subsequently analyzed using the Java-based glycan analysis software glyXtool™ (glyXera, Germany) [56]. By patented normalization to an internal standard, electropherograms were transformed to "*N*-glycan fingerprints" with an excellent long-term migration time reproducibility [5,54]. This allowed automated peak picking, integration and relative quantification, but also structural assignment of *N*-glycan peaks by migration time matching to an in-house *N*-glycan database, containing more than 300 *N*-glycan entries [6,10,50].

To confirm *N*-glycan sequences and linkages, exoglycosidase digests were performed using the enzymes α(2-3) sialidase (SiaS), α(2-3,6,8) sialidase (SiaA), α(1-3,4) fucosidase (a34FUCase), α(1-2,3,4,6) fucosidase (aFUCase), β(1-4) galactosidase (b14GALase), α(1-2,3,6) mannosidase (aMANase) and β(1-2,3,4,6)-*N*-Acetylglucosaminidase (bNAcGLUase). Exoglycosidase digestions were performed under reaction conditions recommended by the suppliers. All enzymes were carefully tested for reactivity and specificity by incubation with APTS labeled *N*-glycans derived from bovine fetuin (for SiaA, SiaS), bovine IgG (for aFUCase, b14GALase and bNAcGLUase), bovine ribonuclease B (for aMANase) and human lactotransferrin (for a34FUCase) (data not shown).

2.7. Statistics

All samples were analyzed in a randomized sequence. Due to the high reproducibility of the method no batch correction had to be performed. Relative peak height proportion (rPHP), standard deviations (SD) and coefficients of variation (CV) were calculated as published in [57]. The horizontal line within the box plot (see Figs. 3–5) indicates the median, boundaries of the box mark the upper and lower quartile (Q1 = 25%, Q3 = 75%, Box = interquartile range (IQR)). The whiskers indicate Q1 − (1.5xIQR) and Q3 + (1.5xIQR). The mean value is illustrated by a square within the box. Normality of distribution was checked by a Kolmogorov–Smirnov test using Origin 8.6.0. Because of non-normal distribution found with some variables, for the comparison of two groups a nonparametric Mann–Whitney U-test was performed using Origin 8.6.0. p-Values <0.05 were considered to be statistically significant.

3. Results

3.1. Subject characteristics and longitudinal sampling procedure

To minimize the variability and the effect of environmental factors in this study, plasma samples were longitudinally collected from individuals of the same gender and age, sharing a very similar lifestyle. In contrast to the design of other studies, where the plasma *N*-glycosylation was evaluated for a big number of individuals at only one time point, this study focuses on the evaluation of the long-term stability of the plasma *N*-glycosylation, collecting samples of a small number of individuals at multiple time points over a long period of time. During this longitudinal sampling, 135 EDTA-plasma samples were collected from five healthy volunteers (V1, V2, V3, V4 and V5) within a timeframe of 1.5 up to six years (V1: n = 22, t = 2 yrs.; V2: n = 29, t = 1.5 yrs.; V3: n = 31, t = 2 yrs.; V4: n = 22, t = 1.5 yr.; V5: n = 31; t = 6 yrs.).

3.2. Refined peak annotation of native and asialo human plasma N-glycome

The native human plasma *N*-glycome was generated by releasing *N*-glycans from frozen normal control plasma using PNGase F. Released *N*-glycans were treated and subjected to xCGE-LIF based glycoanalysis as described above. The asialo human plasma *N*-glycome was generated by SiaA treatment of native plasma *N*-glycome before xCGE-LIF measurement. The 31 most abundant peaks of the native *N*-glycan fingerprint, respectively the 21 most abundant peaks for the asialo *N*-glycan fingerprint, were picked as shown in Fig. 1. Peaks were annotated via *N*-glycan database matching, as described above. To confirm these structural assignments various exoglycosidase digests were performed using SiaS, SiaA, a34FUCase, aFUCase, b14GALase, aMANase, bNAcGLUase, as exemplarily shown in Fig. S1. Compared to previous publications [6,23,41,47], a refinement of the peak annotation was achieved for the native and asialo plasma *N*-glycome. Annotated *N*-glycans, which contribute a substantial proportion to the peak height, are given in Table 1.

The high resolution of xCGE-LIF allows to differentiate between terminal α(2-3) and α(2-6) linked *N*-acetylneuraminic acids (e.g. Fig. 1 and Table 1: peak 2 vs. 3, peak 4 vs. 6 and peak 7 vs. 9 vs. 10), as well as between α(1-6) linked core fucose and α(1-3) linked antenna fucose (e.g. Fig. 1 and Table 1: peak 17 vs. 18, peak XI vs. XII and peak XVI vs. XVII). Hence, this feature even enables the identification of *N*-glycans with $Lewis^X$ and $Sialyl\text{-}Lewis^X$ motifs (e.g. Fig. 1 and Table 1: peaks 5, 8, 16 and peaks XI, XVI, XVIII).

3.3. Precision of the glycoanalytical procedure

To evaluate the reproducibility of the method, respectively to determine the variability associated with the sample preparation, the whole analytical procedure (*N*-glycan release, APTS labeling, HILIC-SPE and xCGE-LIF measurement) was repeated independently 10 times (on different days), by different persons, in different labs, in technical triplicates, using frozen normal control plasma. The 31 most abundant peaks of the *N*-glycan fingerprints of the native human plasma *N*-glycome were picked by glyXtool™ and their rPHPs were calculated as published by Kottler et al. [57]. Averages, SDs and CVs of those rPHPs are given in Table 2. While the biggest rPHP CV for low abundant peaks (<0.5% rPHP) is up to 11%, the rPHP CV for medium to high abundant peaks (>2.5% rPHP) is only up to 3%. The average rPHP CV for all peaks is only about 5.4%, which demonstrates the good reproducibility of the method. Furthermore, the rPHP reproducibility of the xCGE-LIF measurement was evaluated, running the same sample 40 times within the timeframe of one year. An average rPHP CV of 1.7% (Table S1) shows the very high reproducibility of the xCGE-LIF measurement, in spite of the use of different batches of separation polymer and capillary arrays.

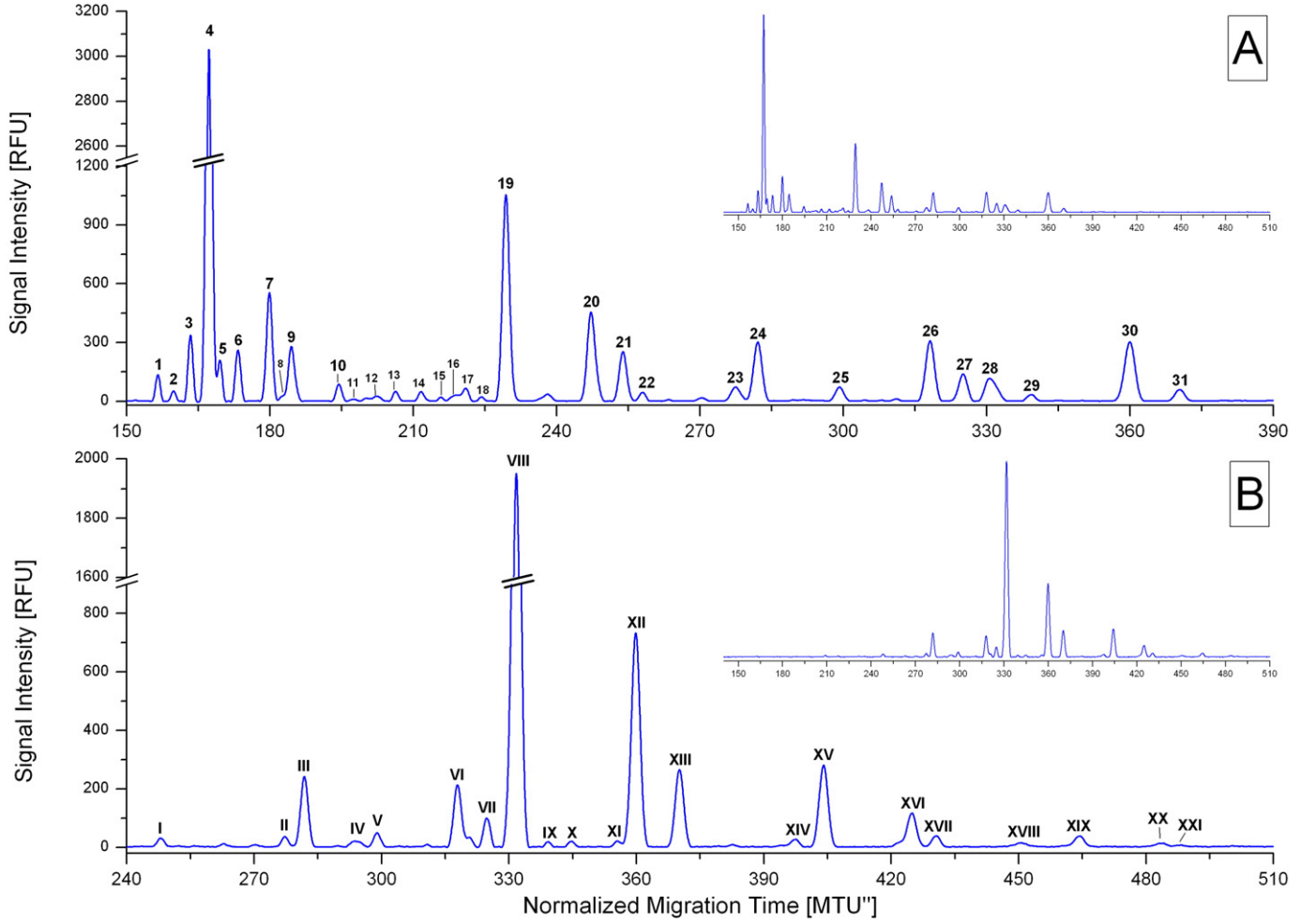

Fig. 1. xCGE-LIF generated human plasma *N*-glycan fingerprints. Signal intensity in relative fluorescence units [RFU] is plotted over the normalized migration time [MTU″]. A — Fingerprint of native (sialylated) frozen normal control plasma-derived *N*-glycome, labeled with APTS and analyzed by xCGE-LIF. B — Fingerprint of desialylated frozen normal control plasma-derived *N*-glycome, labeled with APTS and analyzed by xCGE-LIF. Numbers indicate the 31, respectively the 21 most abundant *N*-glycan peaks, picked within the *N*-glycan fingerprints. The annotation of the picked peaks can be found in Table 1. The inset (subfigures in A and B) show the entire migration time range of the xCGE-LIF measurement.

3.4. Variation of the native human plasma N-glycome between and within individuals

To determine the variability of the human plasma *N*-glycosylation 135 samples from five volunteers were analyzed using the described xCGE-LIF workflow. The 31 most abundant peaks within the *N*-glycan fingerprints of native human plasma *N*-glycomes were picked and their rPHPs, as well as their SDs were calculated. The results were grouped per volunteer and compared in Fig. 2 (data in Table S2). While the variation for a single person over several years is intriguingly small, the difference between the volunteers is rather big. For instance, the average rPHP over time of peak 4 for V1 is 37% (SD: 3%), whereas the average rPHP over time for the same peak for V5 is only 27% (SD: 4%). Comparing the rPHP over time for all volunteers, a lower degree of sialylation can be observed for V5. Peak 4, mainly composed of A2G2S2(2,6) (see Table 1), reveals to be quite small for V5, whereas its partially sialylated (A2G2S1(2,6), peak 19) and non-sialylated (A2G2, peak 28) forms are rather big. The same holds true for A3G3S3 (peak 2) and its partially sialylated counterpart A3G3S2 in peaks 13, 14 and 15.

To determine the seasonal variation and the long-term stability of the human plasma *N*-glycosylation, the 135 samples from five volunteers were grouped and sorted by date. To give an overview, in Fig. 3 the rPHPs of three peaks, comprising a low, middle and high abundant *N*-glycan, were plotted against the time. For the sake of clarity, the time course is only shown for V3 (blue circles) and V5 (red squares). For both volunteers no seasonal trends are visible within the timeframe of one year. Furthermore, the rPHPs of all three peaks are remarkably stable over several years. However, despite this long-term stability, the box plots of the two volunteers show different variabilities. The rPHPs of V5 show a smaller variability than the rPHPs of V3, although the variability of a single volunteer over time is always far below the variability of the entire group (indicated by the three box plots in Fig. 3).

3.5. Influence of environmental factors on the native human plasma N-glycome of individuals

For each volunteer the parameters illness, allergy, sleep behavior, as well as food and alcohol consumption were carefully documented, to investigate the influence of lifestyle and environmental factors on human plasma *N*-glycome variability of an individual over time. To establish a relationship between event and response, all samples of one event of a volunteer over time were grouped and compared to the group of its counterpart out of his time series (e.g. common cold vs. healthy status or normal sleep vs. lack of sleep). A sample was assigned to a certain group only, if the event (e.g. sports injury) took place max. two days before sampling. The statistical significances between groups were evaluated by a Mann–Whitney U test for all 31 *N*-glycan peaks of the

Table 1
N-glycan structures assigned to the peaks of the native and asialo human plasma *N*-glycan fingerprint of Fig. 1.
Symbolic representation of *N*-glycan structures were drawn with GlycoWorkbench Version 1.1, following the guideline of the Consortium for Functional Glycomics [58]. Glycan names are based on Oxford nomenclature (modified to our needs). The 31, respectively 21 most abundant peaks inside the native, or asialo human plasma *N*-glycome fingerprint were annotated via *N*-glycan database matching and confirmed by various exoglycosidase digests, using SiaS, SiaA, a34FUCase, aFUCase, b14GALase, aMANase, bNAcGLUase.

Peak	*N*-glycan name	*N*-glycan structure	Peak	*N*-glycan name	*N*-glycan structure
1	A4G4S4(2,6)		I	Man5	
2	A3G3S3(2,6)		II	Man6	
3	A3G3S1(2,3)S2(2,6)		III	FA2G0 FA1G1[6]	
4	A2G2S2(2,6)		IV	FA1G1[3]	
5	A3F(3)G3S1(2,3)S2(2,6)	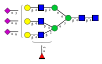	V	FA2BG0	
6	A2G2S1(2,6)S1(2,3)		VI	FA2G1[6]	
7	FA2G2S2(2,6)		VII	FA2G1[3]	
8	A2F(3)G2S1(2,6)S1(2,3)	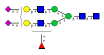	VIII	A2G2 FA2BG1[6]	
9	FA2BG2S2(2,6) FA2G2S1(2,3)S1(2,6)		IX	Man8 FA2BG1[3]	
10	FA2G2S2(2,3) A4G4S2(2,3)S1(2,6)	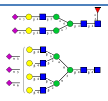	X	A2BG2	
11	FA1G1S1(2,6)[3] FA1G1S1(2,3)[6] A2G1S1(2,6)[6]	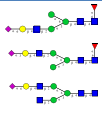	XI	A2F(3)G2	
12	A2G1S1(2,6)[3] A4F(3)G4S1(2,3)S2(2,6)	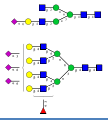	XII	FA2G2 Man9	
13	A3G3S2(2,6)		XIII	FA2BG2	
14	A3G3S1(2,3)S1(2,6)		XIV	A3G3[2,6]	
15	A3G3S1(2,3)S1(2,6)		XV	A3G3[2,4]	
16	A3F(3)G3S2(2,6)	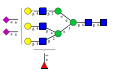	XVI	A3[2,4]F(3)G3	
17	FA2G1S1(2,6)[3] FA3G3S2(2,6)	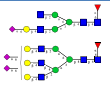	XVII	FA3[2,4]G3	
18	A3F(3)G3S1(2,3)S1(2,6) FA2G1S1(2,3)[6] FA2BG1S1(2,6)[6]	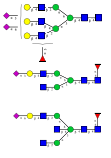	XVIII	FA3[2,4]F(3)G3	

Table 1 (*continued*)

19	A2G2S1(2,6) FA2BG1S1(2,6)[3]	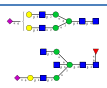	XIX	A4G4	
20	FA2G2S1(2,6) Man5	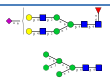	XX	A4F(3)G4	
21	FA2BG2S1(2,6) FA2G2S1(2,3)[6]		XXI	FA4G4	
22	FA2G2S1(2,3)[3]				
23	Man6				
24	FA2G0 A3G3S1(2,6)				
25	FA2BG0				
26	FA2G1[6]				
27	FA2G1[3]				
28	A2G2 FA2BG1[6]				
29	Man8 FA2BG1[3]				
30	FA2G2 Man9				
31	FA2BG2				

native *N*-glycan fingerprint, as well as for various *N*-glycan classes and subclasses (Table S3). *N*-glycan classes and subclasses were built based on *N*-glycan properties, like neutral, sialylated, bisected, core fucosylated, biantennary and triantennary. A complete list of *N*-glycan classes and subclasses and their associated peaks can be found in Table S4.

E.g., V4 had several sport injuries during the sampling period. To evaluate the influence of this factor on the plasma *N*-glycome, the V4 sports injury samples over time were compared to his healthy control samples out of his time series. In case of sports injury the proportion of sialylated *N*-glycans increased significantly from 79.4% to 81.2% (Fig. 4B), while the proportion of neutral *N*-glycans inside the *N*-glycan fingerprint dropped significantly from 19.4% to 17.6% (Fig. 4A). But, comparing the V4 sports injury sample group with the group of all healthy volunteers over time, no significant changes can be observed (Fig. 4A and B, blue box plot). To evaluate if the subclasses of neutral *N*-glycans are affected by sports injury, the change of fucosylated and bisected *N*-glycans was plotted in Fig. 4C and D. Apparently, both subclasses are showing the same trend, a significant decrease in case of the sports injury. Besides this, also an influence of sports injury on the degree of galactosylation could be found. While the ratio of FA2G0 to neutral complex *N*-glycans (Peak 24/sum(Peaks 24–31)) decreased with $p < 0.05$, the ratio of the FA2G2 to neutral complex *N*-glycans (Peak 30/sum(Peaks 24–31)) increased slightly with $p < 0.05$ (see Table S3), indicating a raised galactosylation after sports injury.

Table 2
Precision of the glycoanalytical procedure. Frozen normal control plasma was independently analyzed (*N*-glycan release, labeling, purification and xCGE-LIF measurement) at 10 different days, each time in technical triplicates (n = 30). Within the xCGE-LIF generated native plasma *N*-glycan fingerprints the 31 most abundant peaks were picked and their relative peak height proportions (rPHP) were calculated. To evaluate the precision of the analytical procedure, the average rPHP was calculated for each peak, as well as its standard deviation (SD) and its coefficient of variation (CV).

Peak no.	rPHP in %	SD	CV in %
1	1.80	0.06	3.11
2	0.83	0.07	8.56
3	4.62	0.13	2.76
4	37.11	0.47	1.26
5	2.86	0.11	3.76
6	3.44	0.08	2.33
7	6.66	0.25	3.81
8	0.37	0.04	10.36
9	3.21	0.13	3.91
10	1.13	0.03	2.70
11	0.18	0.02	11.20
12	0.28	0.03	11.29
13	0.57	0.03	4.80
14	0.60	0.04	7.39
15	0.30	0.03	9.20
16	0.40	0.04	11.02
17	0.82	0.04	4.64
18	0.31	0.03	11.21
19	11.33	0.36	3.14
20	4.96	0.14	2.83
21	2.57	0.07	2.62
22	0.56	0.02	4.00
23	0.85	0.03	3.07
24	3.60	0.21	5.89
25	0.80	0.04	5.51
26	3.28	0.20	6.25
27	1.54	0.10	6.49
28	1.16	0.05	4.18
29	0.37	0.01	3.76
30	2.93	0.13	4.40
31	0.56	0.02	3.32
	Average rPHP CV:		5.44

In a second example the influence of a common cold on the native human plasma *N*-glycan composition is shown. V5 suffered several times from a common cold during the sampling period, resulting in a significant decrease of diantennary plasma *N*-glycans (Fig. 5A) and a significant increase of triantennary plasma *N*-glycans (Fig. 5B). Apparently, suffering from a pollen allergy had the same effect on the plasma *N*-glycan composition of V5, decreasing the level of diantennary *N*-glycans (Fig. 5C) and increasing the level of triantennary plasma *N*-glycans (Fig. 5D).

4. Discussion

Since for large-scale biomarker discovery studies usually plasma *N*-glycosylation is evaluated for samples taken from a large number of individuals but only at one time point [21–23,35,42,44,46,47], the questions arise: "Are disease caused changes really significant compared to the differences between individuals, and how representative is a single sample taken from one person at only one time point, respectively, how stable is the *N*-glycome of a person over time?" Gornik et al. proved in 2009 that everyday activities have no global effects on the protein *N*-glycosylation of human plasma, attesting a high intraday and interday stability of the plasma *N*-glycome [48]. Nevertheless, the influence of weekly, monthly or seasonal events on the plasma *N*-glycome stability was not evaluated by them. Thus, to estimate the diagnostic potential of the plasma *N*-glycome as a biomarker, we monitored its long-term stability over a time period of up to six years, by collecting samples of a small number of individuals, but at multiple time points.

In order to properly assess the results of our long-term stability study we initially determined the precision of the analytical procedure by a reproducibility test. Therefore, a sample was analyzed independently 10 times in triplicates (Table 2). The obtained average rPHP CV of 5.4% indicates a high precision of the analytical procedure, which is absolutely comparable with other state-of-the-art *N*-glycan analysis techniques [59] (HILIC-HPLC: 4.3% [45], MALDI-TOF: below 6% or 8% [60], HPLC-MS: below 5% [61]). In particular, repeated xCGE-LIF based measurements with an average rPHP CV of only 1.7% (Table S1) are demonstrating its high reproducibility and competitiveness. This further indicates that sample preparation is the major origin of variation of the method.

To evaluate variability, respectively, the long-term stability of the native human plasma *N*-glycome, we analyzed samples of five healthy volunteers collected in a timeframe of up to six years (Fig. 2 and Table S2). The long-term stability measured by the average rPHP CV of all peaks was between 8.5% (analyzing 31 samples collected over six years from V5) to 11.4% (analyzing 31 samples collected over two years from V3). This surprisingly small variability, which was only slightly above the variability of the analytical procedure, demonstrates the impressive long-term stability of individual human plasma *N*-glycomes. However, the variability was not equally distributed over all peaks. Notably, for all volunteers peaks 2, 11 and 15 show a higher rPHP variability, and thus are indicating that the underlying *N*-glycan structures are probably stronger regulated and quite sensitive to lifestyle and environmental factors (Table S2). This variability might reflect changes in concentration of certain plasma proteins, which still need to be determined. In contrast, the rPHPs of neutral complex *N*-glycans (peaks 24–31, mainly related to IgG [16]) are quite stable, or rather insensitive to environmental factors. While the temporal variability of the *N*-glycome of a single volunteer was shown to be rather small over several years, the differences between the individuals can be remarkably big (see Figs. 2 and 3). Due to the fact that all volunteers share quite similar features (e.g. gender, age and lifestyle), this big differences in the *N*-glycome can only be explained by a strong influence of the genetic background. This finding is consistent with the study of Knezevic et al. analyzing the plasma *N*-glycome of 1008 individuals [45]. In contrast, the difference in rPHP between the volunteers are smaller for the asialo *N*-glycome (Table S5), indicating the influence of sialylation as a major contributor of variability. A performed GlycoAge Test on the asialo *N*-glycome resulted in values from −0.4 to −0.5 for all volunteers (Table S5), which is in good agreement with the previously published values of a healthy Belgian population [52].

Finally, we attempted to identify the origin of the *N*-glycome variability. To visualize whether the plasma *N*-glycome undergoes seasonal fluctuations, the rPHPs of three selected peaks were plotted over the time for V3 and V5 (Fig. 3). Apparently, these representative examples show no significant seasonal fluctuations of the *N*-glycome. To evaluate whether the small observed variability is caused by certain events like illness or allergy, we performed a correlation analysis of the documented lifestyle and environmental factors with the changes in the human plasma *N*-glycome. V4 had several sport injuries during the sampling period, associated with sprain and bruises of joints, thus local inflammation. It is known that a large number of blood glycoproteins are synthesized by the liver and B-lymphocytes [8,16], hence changes in the serum total *N*-glycan compositions could reflect an alteration of the liver or B-lymphocyte physiology [23]. Nevertheless, as a response to local and systemic inflammation (e.g. a septic shock), the liver produces a large number of acute-phase proteins, secreted into the bloodstream. These acute-phase proteins are highly sialylated [13,16], increasing the overall percentage of sialylated *N*-glycans inside the blood plasma [62,63]. Apparently, as displayed in Fig. 4, this is consistent with observations for V4. In case of sports injury the proportion of sialylated *N*-glycans increased significantly (Fig. 4B), while the proportion of neutral *N*-glycans decreased significantly (Fig. 4A). Although both effects are small, the grouped sports injury samples of V4 can be clearly separated

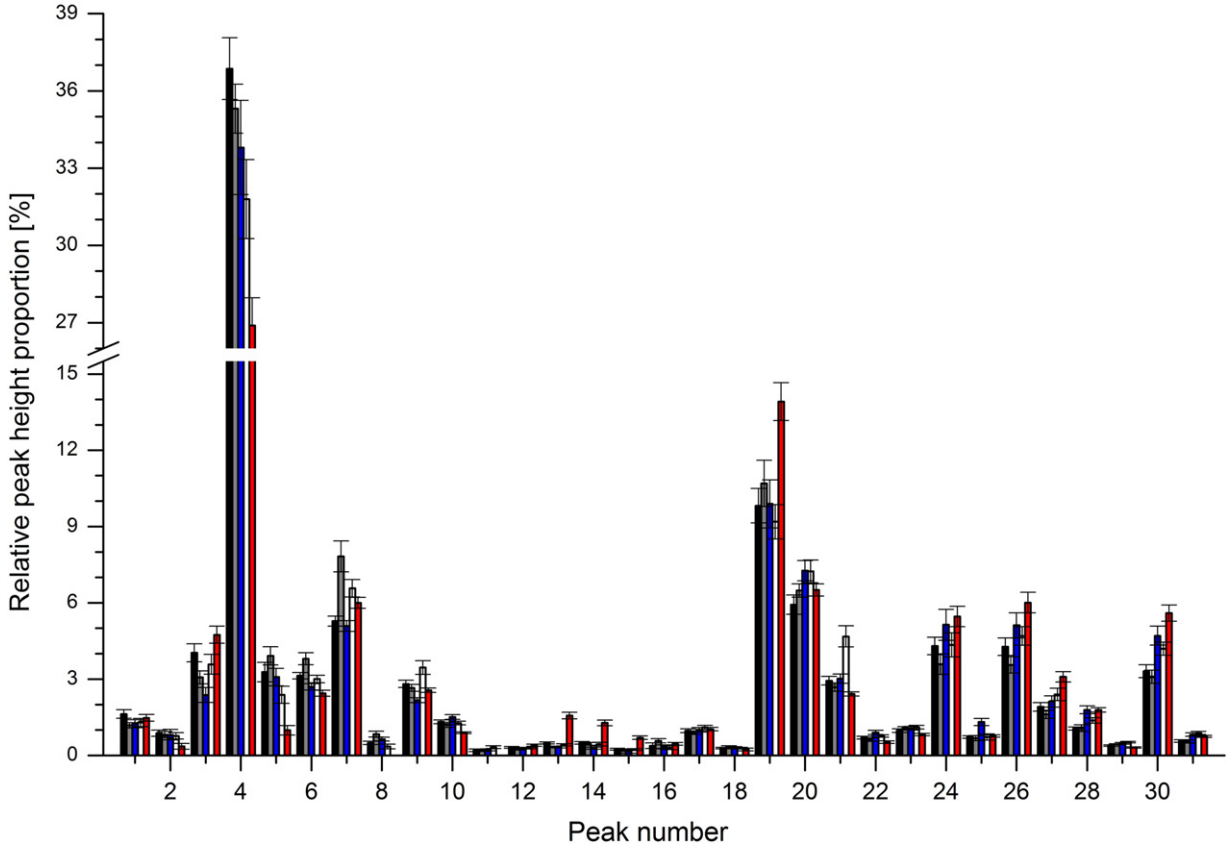

Fig. 2. Bar plot for the comparison of the average relative peak height proportions (rPHP) from five individuals over time. To evaluate the variation of human plasma *N*-glycome between individuals, the native human plasma *N*-glycome of in total 135 samples was analyzed. Samples, originated from five healthy volunteers (V1–V5), were sampled over a time period of at least one year (V1 (black): n = 22, t = 2 yrs.; V2 (gray): n = 29, t = 1.5 yrs.; V3 (blue): n = 31, t = 2 yrs.; V4 (white): n = 22, t = 1 yr.; V5 (red): n = 31; t = 6 yrs). from the generated *N*-glycan fingerprints the 31 most abundant peaks were picked and its rPHPs were calculated. For the bar plot all longitudinal samples of one volunteer were grouped and the average rPHP, as well as its SD were calculated. For example, peak 4 of volunteer 5 (red) had an average rPHP (i.e. a relative abundance) of 27% over six years, with a SD of 4% (exact values can be found in Table S2). One representative xCGE-LIF generated human plasma *N*-glycan fingerprint of each volunteer, as well as an overlay of those, can be found in supplementary Fig. S2.

from the healthy control samples with $p < 0.01$ of V4. However, due to a large variability between individuals, the sports injury group cannot be separated from the healthy control group comprising the data from all five volunteers (Fig. 4A, red vs. blue box plot). This could explain why glycan biomarkers from large-scale studies, where samples are taken from a large number of individuals — but only at one time point, often have only a limited specificity. Furthermore, a small, but significant increase of the galactosylation degree could be observed in case of sports injury (Table S3). Since a big proportion of the neutral complex *N*-glycans in human plasma are derived from IgG [16], an increase of the galactosylation presumably implies an increase of IgG galactosylation, which is described in literature to have an anti-inflammatory/immunosuppressive function [40,64]. In a second example V5 suffered several times during the sampling period from a common cold. A significant decrease of diantennary *N*-glycans and significant increase of triantennary *N*-glycans could always be observed in case of illness (see Fig. 5). The origin of this effect can only be explained by identifying triantennary *N*-glycans-containing plasma proteins and looking at their functions. In the review of Clerc at al. [16] alpha-1-acid glycoprotein (AGP) and alpha-1-antitrypsin (AAT) are declared to be one of the main contributors of triantennary *N*-glycans in the human plasma *N*-glycome. Both proteins are mainly produced by the liver, being involved in the defense of the body against respiratory infections. For example AGP is an acute-phase protein, known as a negative modulator of inflammation, whereas AAT acts as inhibitor of a wide range of serine proteases. Due to its small size and its hydrophilicity AAT can easily move into tissue fluids, such as mucus of lungs, preventing the proteolytic destruction of the lower respiratory tract [65]. Hence, the higher production of AAT and AGP as a response to the inflammation of respiratory tract during the common cold could be an explanation for the increased levels of triantennary plasma *N*-glycans.

In both examples a significant change over time in the composition of the plasma *N*-glycome of one individual could be detected. In case of sports injury (Fig. 4), the disease related changes are small and not significant compared to the healthy control group. Consequently, due to the big inter-individual differences, small but significant changes might have been undetected, when looking only at a single time point of a large cohort. The second case shows a different characteristic. A significant decrease of diantennary *N*-glycans during a common cold could be observed for V5 ($p < 0.05$), as well as for the healthy control group ($p < 0.01$) (Fig. 5A). However, a significant decrease of diantennary *N*-glycans could also be observed comparing the healthy status of V5 with the healthy control group ($p < 0.01$). This means, the already low status of diantennary *N*-glycans in plasma of V5 (see Table S5) results in a false positive detection of a healthy V5 as diseased. The same holds true for the triantennary *N*-glycans during a common cold for V5 (Fig. 5B), due to naturally elevated levels of triantennary plasma *N*-glycans for V5.

5. Conclusion and outlook

Here, we present a sophisticated method to analyze the human plasma *N*-glycome, based on xCGE-LIF. The straightforward sample preparation, in a 96 well format in combination with the multi-capillary gel electrophoresis system, enables the analysis of hundreds of samples in real high throughput. Due to the high sensitivity

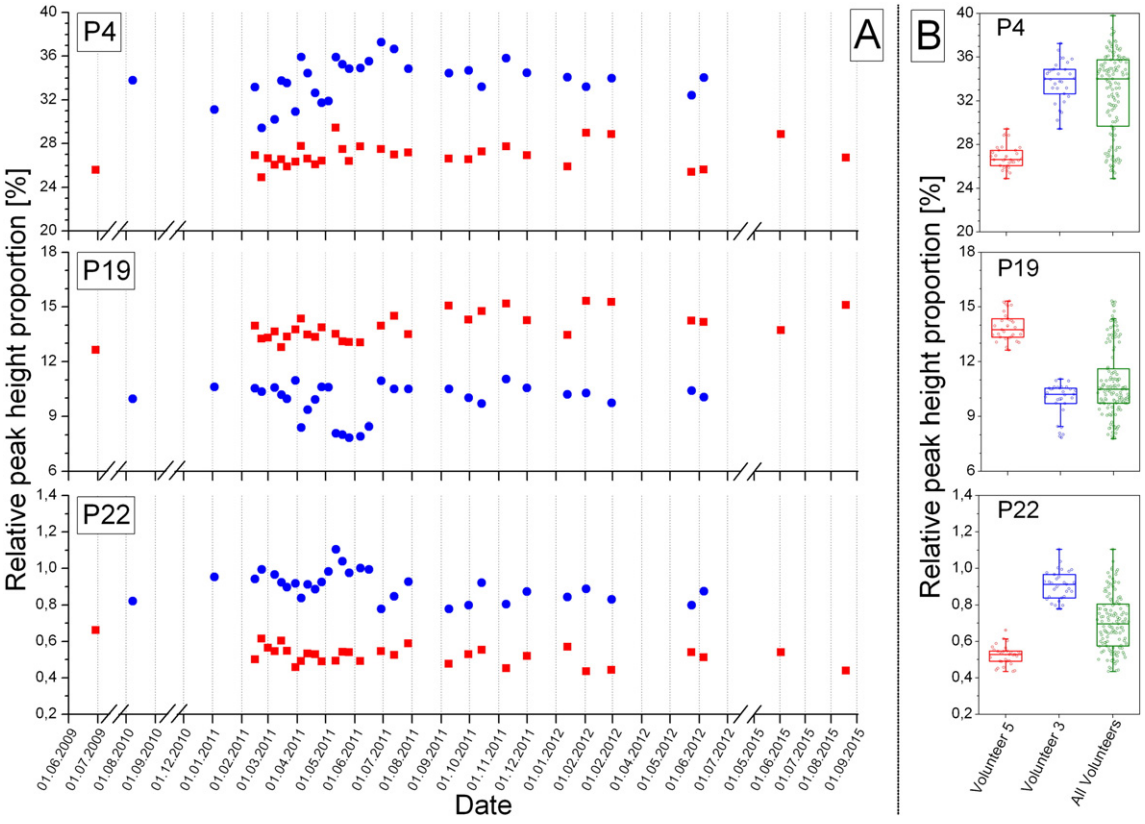

Fig. 3. Evaluation of the intra-individual and inter-individual variability of the plasma *N*-glycome. A — To illustrate the variability of human plasma *N*-glycome within individuals (intra-individual variability), exemplarily the rPHP of three peaks (high, middle and low abundant) was plotted over the sampling time points (volunteer 3—blue circles; volunteer 5—red squares). An overlay of the native plasma-derived *N*-glycome fingerprints of volunteer 5 can be found in supplementary Fig. S3. B — Comparison of the intra-individual (one donor: V3, middle box plot; V5, left box plot) with the inter-individual (all donors, right box plot) variability of the *N*-glycome. The box plot was generated by including the rPHP of all sampling time points (V3 and V5: n = 31; all volunteers: n = 135), thereby each sample is represented as a circle inside the box plot. Parameters of the box plot visualization (e.g. boundaries and whiskers) are defined within the "Statistics" section. Underlying data, as well the data of all other volunteers can be found in Table S2.

of xCGE-LIF, a minimal invasive sampling could be applied, taking only a single droplet of capillary blood from a fingertip. The superior resolution of the xCGE-LIF measurement and a refined peak annotation for the native and asialo plasma *N*-glycome, will enable to monitor a bigger number of *N*-glycan motifs (like Lewis^X and Sialyl-Lewis^X) in the future.

Via a long-term stability study of the native plasma *N*-glycome, it could be demonstrated that the individual's *N*-glycome is remarkably stable over a period of several years and independent from seasons. Furthermore, it could be demonstrated that the inter-individual differences of the *N*-glycome are enormous, but by looking at the progression of the plasma *N*-glycome of a single person, small changes could be detected and linked to lifestyle and environmental factors. Consequently, taking time-series from individuals can be beneficial compared to large-scale studies, where samples are taken from a large number of donors (but only once). In such cross-sectional studies, small disease related changes in the *N*-glycome would be hidden within the population variation, caused by the inter-individual differences of the *N*-glycome.

Our future aim is to further evaluate and validate these initial results with longitudinal studies of larger sample cohorts. Especially, the influence of various environmental factors on the plasma *N*-glycome needs to be evaluated, leading to personalized longitudinal plasma *N*-glycan fingerprints (plPNF), which contain information about the individual "normal" *N*-glycan composition in combination with its longitudinal variability. Subsequently, this information could be used to detect even small disease associated temporal changes in glycosylation, which are above the individual longitudinal variability of the plPNF. Finally, this will increase the predictive strength of glycan biomarkers, making them to a powerful tool in personalized diagnostics.

Supplementary data to this article can be found online at http://dx.doi.org/10.1016/j.bbagen.2016.03.035.

Transparency document

The Transparency document associated with this article can be found, in online version.

Acknowledgments

RH, MH, RK and ER acknowledge support by the European Union (EC) under the project "HighGlycan" (grant no. 278535). SC and ER acknowledge support by the German Federal Ministry of Education and Research (BMBF) under the project "Die Golgi Glykan Fabrik 2.0" (grant identifier 031A557). ER acknowledges support by the European Union (EC) under the project "HTP-GlycoMet" (grant no. 324400). The authors thank Veronika Wank for technical assistance.

Patient consent statement

All volunteers signed informed consent before participating in the study.

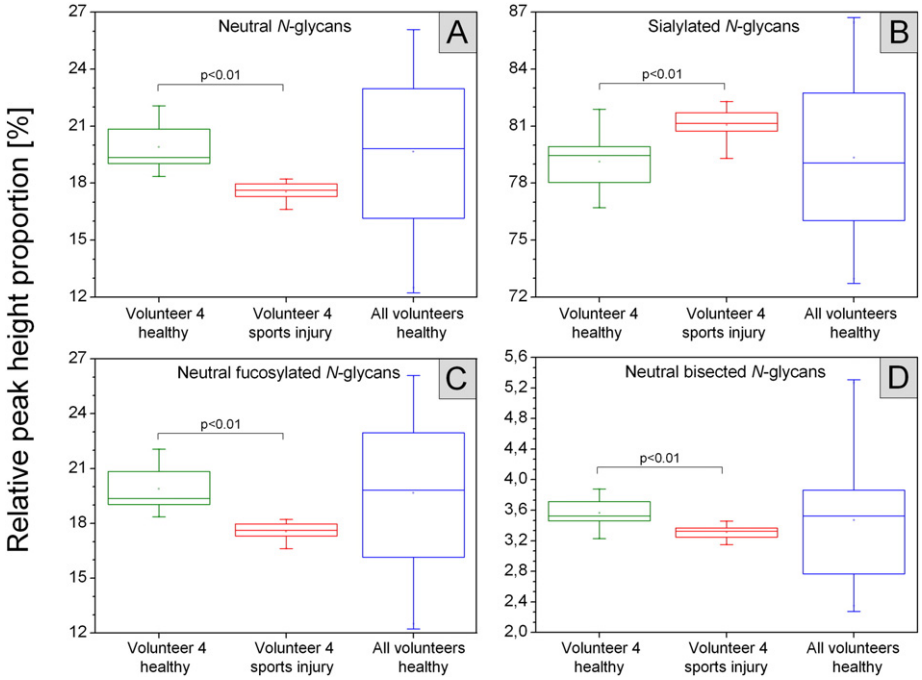

Fig. 4. Injury-related changes in the abundance of different *N*-glycan classes and subclasses for volunteer 4. All samples of volunteer 4, each time taken after a sports injury (red box plot, n = 7), were grouped and compared to the healthy control samples of volunteer 4 (green box plot, n = 15), and to the healthy control samples of all volunteers (blue box plot, n = 100). A — Box plots of the neutral complex *N*-glycan class (sum of peaks 24–31). B — Box plots of the sialylated complex *N*-glycan class (sum of peaks 1–22). C — Box plots of the neutral fucosylated complex *N*-glycan subclass (sum of peaks 24–31). D — Box plots of the neutral bisected complex *N*-glycan subclass (sum of peaks 25, 28, 29, 31). Parameters of the box plot visualization (e.g. boundaries and whiskers) are defined within the "Statistics" section. The underlying data can be found in Table S3.

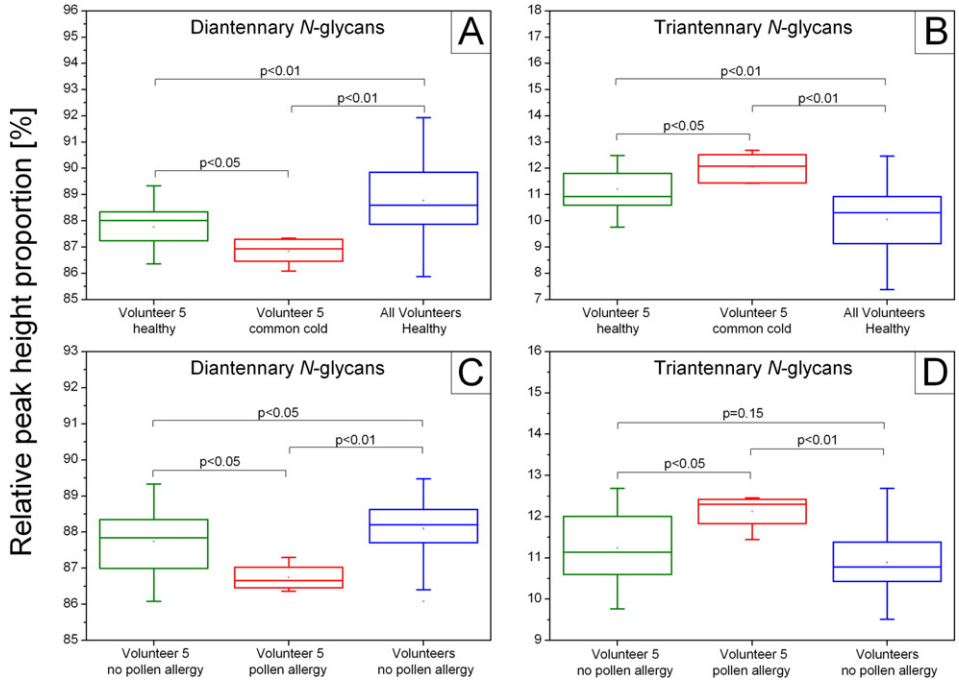

Fig. 5. Common cold and pollen allergy related changes in the abundance of different *N*-glycan classes for volunteer 5. All samples of volunteer 5, taken during a common cold (A and B: red box plots, n = 6) and during pollen allergy (C and D: red box plots, n = 4) were grouped and compared to the healthy control samples of volunteer 5 (A and B: green box plots, n = 25; C and D: green box plots, n = 27), and to the healthy control samples of all volunteers (A–D blue box plots, n = 100). A and C — Box plots of the diantennary complex *N*-glycan class (sum of peaks 4, 6–12, 17–22, 24–31). B and D — Box plots of the triantennary complex *N*-glycan class (sum of peaks 2, 3, 5, 13–18). Parameters of the box plot visualization (e.g. boundaries and whiskers) are defined within the "Statistics" section. The underlying data can be found in Table S3.

References

[1] K. Landsteiner, Ueber Agglutinationserscheinungen normalen menschlichen Blutes, Wien. Klin. Wochenschr. 14 (1901) 1132–1134.
[2] W.M. Watkins, The ABO blood group system: historical background, Transfus. Med. 11 (2001) 243–265.
[3] W. Laroy, R. Contreras, N. Callewaert, Glycome mapping on DNA sequencing equipment, Nat. Protoc. 1 (2006) 397–405.
[4] L. Royle, M.P. Campbell, C.M. Radcliffe, D.M. White, D.J. Harvey, J.L. Abrahams, Y. Kim, G.W. Henry, N.A. Shadick, M.E. Weinblatt, D.M. Lee, P.M. Rudd, R.A. Dwek, HPLC-based analysis of serum N-glycans on a 96-well plate platform with dedicated database software, Anal. Biochem. 376 (2008) 1–12.
[5] J. Schwarzer, E. Rapp, U. Reichl, N-glycan analysis by CGE–LIF: profiling influenza A virus hemagglutinin N-glycosylation during vaccine production, Electrophoresis 29 (2008) 4203–4214.
[6] L.R. Ruhaak, R. Hennig, C. Huhn, M. Borowiak, R.J.E.M. Dolhain, A.M. Deelder, E. Rapp, M. Wuhrer, Optimized workflow for preparation of APTS-labeled N-glycans allowing high-throughput analysis of human plasma glycomes using 48-channel multiplexed CGE-LIF, J. Proteome Res. 9 (2010) 6655–6664.
[7] D. Vanderschaeghe, A. Szekrenyes, C. Wenz, M. Gassmann, N. Naik, M. Bynum, H. Yin, J. Delanghe, A. Guttman, N. Callewaert, High-throughput profiling of the serum N-glycome on capillary electrophoresis microfluidics systems: toward clinical Implementation of GlycoHepatoTest, Anal. Chem. 82 (2010) 7408–7415.
[8] R.S. Tirumalai, K.C. Chan, D.A. Prieto, H.J. Issaq, T.P. Conrads, T.D. Veenstra, Characterization of the low molecular weight human serum proteome, Mol. Cell. Proteomics 2 (2003) 1096–1103.
[9] D.F. Zielinska, F. Gnad, J.R. Wisniewski, M. Mann, Precision mapping of an in vivo N-glycoproteome reveals rigid topological and sequence constraints, Cell 141 (2010) 897–907.
[10] J.E. Huffman, M. Pučić-Baković, L. Klarić, R. Hennig, M.H.J. Selman, F. Vučković, M. Novokmet, J. Krištić, M. Borowiak, T. Muth, O. Polašek, G. Razdorov, O. Gornik, R. Plomp, E. Theodoratou, A.F. Wright, I. Rudan, C. Hayward, H. Campbell, A.M. Deelder, U. Reichl, Y.S. Aulchenko, E. Rapp, M. Wuhrer, G. Lauc, Comparative performance of four methods for high-throughput glycosylation analysis of immunoglobulin G in genetic and epidemiological research, Mol. Cell. Proteomics 13 (2014) 1598–1610.
[11] M. Hoffmann, K. Marx, U. Reichl, M. Wuhrer, E. Rapp, Site-specific O-glycosylation analysis of human blood plasma proteins, Mol. Cell. Proteomics (2015).
[12] D. Kolarich, B. Lepenies, P.H. Seeberger, Glycomics, glycoproteomics and the immune system, Curr. Opin. Chem. Biol. 16 (2012) 214–220.
[13] T. Liu, W.J. Qian, M.A. Gritsenko, D.G. Camp 2nd, M.E. Monroe, R.J. Moore, R.D. Smith, Human plasma N-glycoproteome analysis by immunoaffinity subtraction, hydrazide chemistry, and mass spectrometry, J. Proteome Res. 4 (2005) 2070–2080.
[14] M. Wuhrer, M.I. Catalina, A.M. Deelder, C.H. Hokke, Glycoproteomics based on tandem mass spectrometry of glycopeptides, J. Chromatogr. B 849 (2007) 115–128.
[15] L.R. Ruhaak, G. Zauner, C. Huhn, C. Bruggink, A.M. Deelder, M. Wuhrer, Glycan labeling strategies and their use in identification and quantification, Anal. Bioanal. Chem. 397 (2010) 3457–3481.
[16] F. Clerc, K.R. Reiding, B.C. Jansen, G.S. Kammeijer, A. Bondt, M. Wuhrer, Human plasma protein N-glycosylation, Glycoconj. J. (2015).
[17] G. Zauner, C.A.M. Koeleman, A.M. Deelder, M. Wuhrer, Mass spectrometric O-glycan analysis after combined O-glycan release by beta-elimination and 1-phenyl-3-methyl-5-pyrazolone labeling, Biochim. Biophys. Acta 1820 (2012) 1420–1428.
[18] U. Lewandrowski, J. Moebius, U. Walter, A. Sickmann, Elucidation of N-glycosylation sites on human platelet proteins: a glycoproteomic approach, Mol. Cell. Proteomics 5 (2006) 226–233.
[19] K.R. Reiding, D. Blank, D.M. Kuijper, A.M. Deelder, M. Wuhrer, High-throughput profiling of protein N-glycosylation by MALDI-TOF-MS employing linkage-specific sialic acid esterification, Anal. Chem. 86 (2014) 5784–5793.
[20] H. Stockmann, R.M. Duke, S. Millan Martin, P.M. Rudd, Ultrahigh throughput, ultrafiltration-based n-glycomics platform for ultraperformance liquid chromatography (ULTRA(3)), Anal. Chem. 87 (2015) 8316–8322.
[21] R. Testa, V. Vanhooren, A.R. Bonfigli, M. Boemi, F. Olivieri, A. Ceriello, S. Genovese, L. Spazzafumo, V. Borelli, M.G. Bacalini, S. Salvioli, P. Garagnani, S. Dewaele, C. Libert, C. Franceschi, N-glycomic changes in serum proteins in type 2 diabetes Mellitus correlate with complications and with metabolic syndrome parameters, PLoS One 10 (2015) e0119983.
[22] S. Albrecht, L. Unwin, M. Muniyappa, P.M. Rudd, Glycosylation as a marker for inflammatory arthritis, Cancer Biomark. 14 (2014) 17–28.
[23] X.E. Liu, L. Desmyter, C.F. Gao, W. Laroy, S. Dewaele, V. Vanhooren, L. Wang, H. Zhuang, N. Callewaert, C. Libert, R. Contreras, C. Chen, N-glycomic changes in hepatocellular carcinoma patients with liver cirrhosis induced by hepatitis B virus, Hepatology 46 (2007) 1426–1435.
[24] K. Noda, E. Miyoshi, N. Uozumi, S. Yanagidani, Y. Ikeda, C. Gao, K. Suzuki, H. Yoshihara, K. Yoshikawa, K. Kawano, N. Hayashi, M. Hori, N. Taniguchi, Gene expression of alpha1-6 fucosyltransferase in human hepatoma tissues: a possible implication for increased fucosylation of alpha-fetoprotein, Hepatology 28 (1998) 944–952.
[25] Y. Sato, K. Nakata, Y. Kato, M. Shima, N. Ishii, T. Koji, K. Taketa, Y. Endo, S. Nagataki, Early recognition of hepatocellular carcinoma based on altered profiles of alpha-fetoprotein, N. Engl. J. Med. 328 (1993) 1802–1806.
[26] D. Vanderschaeghe, W. Laroy, E. Sablon, P. Halfon, A. Van Hecke, J. Delanghe, N. Callewaert, GlycoFibroTest: DNA sequencer-based serum protein glycomics yields a highly performant liver fibrosis biomarker, Mol. Cell. Proteomics 8 (2009) 986–994.
[27] U.M. Abd Hamid, L. Royle, R. Saldova, C.M. Radcliffe, D.J. Harvey, S.J. Storr, M. Pardo, R. Antrobus, C.J. Chapman, N. Zitzmann, J.F. Robertson, R.A. Dwek, P.M. Rudd, A strategy to reveal potential glycan markers from serum glycoproteins associated with breast cancer progression, Glycobiology 18 (2008) 1105–1118.
[28] Z. Kyselova, Y. Mechref, P. Kang, J.A. Goetz, L.E. Dobrolecki, G.W. Sledge, L. Schnaper, R.J. Hickey, L.H. Malkas, M.V. Novotny, Breast cancer diagnosis and prognosis through quantitative measurements of serum glycan profiles, Clin. Chem. 54 (2008) 1166–1175.
[29] L. Harris, H. Fritsche, R. Mennel, L. Norton, P. Ravdin, S. Taube, M.R. Somerfield, D.F. Hayes, R.C. Bast Jr., American Society of Clinical Oncology 2007 update of recommendations for the use of tumor markers in breast cancer, J. Clin. Oncol. Off. J. Am. Soc. Clin. Oncol. 25 (2007) 5287–5312.
[30] M. Nakano, T. Nakagawa, T. Ito, T. Kitada, T. Hijioka, A. Kasahara, M. Tajiri, Y. Wada, N. Taniguchi, E. Miyoshi, Site-specific analysis of N-glycans on haptoglobin in sera of patients with pancreatic cancer: a novel approach for the development of tumor markers, Int. J. Cancer 122 (2008) 2301–2309.
[31] N. Okuyama, Y. Ide, M. Nakano, T. Nakagawa, K. Yamanaka, K. Moriwaki, K. Murata, H. Ohigashi, S. Yokoyama, H. Eguchi, O. Ishikawa, T. Ito, M. Kato, A. Kasahara, S. Kawano, J. Gu, N. Taniguchi, E. Miyoshi, Fucosylated haptoglobin is a novel marker for pancreatic cancer: a detailed analysis of the oligosaccharide structure and a possible mechanism for fucosylation, Int. J. Cancer 118 (2006) 2803–2808.
[32] R. Saldova, L. Royle, C.M. Radcliffe, U.M. Abd Hamid, R. Evans, J.N. Arnold, R.E. Banks, R. Hutson, D.J. Harvey, R. Antrobus, S.M. Petrescu, R.A. Dwek, P.M. Rudd, Ovarian cancer is associated with changes in glycosylation in both acute-phase proteins and IgG, Glycobiology 17 (2007) 1344–1356.
[33] R. Saldova, Y. Fan, J.M. Fitzpatrick, R.W. Watson, P.M. Rudd, Core fucosylation and alpha2-3 sialylation in serum N-glycome is significantly increased in prostate cancer comparing to benign prostate hyperplasia, Glycobiology 21 (2011) 195–205.
[34] J. Bones, J.C. Byrne, N. O'Donoghue, C. McManus, C. Scaife, H. Boissin, A. Nastase, P.M. Rudd, Glycomic and glycoproteomic analysis of serum from patients with stomach cancer reveals potential markers arising from host defense response mechanisms, J. Proteome Res. 10 (2011) 1246–1265.
[35] L.R. Ruhaak, D.A. Barkauskas, J. Torres, C.L. Cooke, L.D. Wu, C. Stroble, S. Ozcan, C.C. Williams, M. Camorlinga, D.M. Rocke, C.B. Lebrilla, J.V. Solnick, The serum immunoglobulin G glycosylation signature of gastric cancer, EuPA Open Proteomics 6 (2015) 1–9.
[36] J.N. Arnold, R. Saldova, M.C. Galligan, T.B. Murphy, Y. Mimura-Kimura, J.E. Telford, A.K. Godwin, P.M. Rudd, Novel glycan biomarkers for the detection of lung cancer, J. Proteome Res. 10 (2011) 1755–1764.
[37] R. Parekh, I. Roitt, D. Isenberg, R. Dwek, T. Rademacher, Age-related galactosylation of the N-linked oligosaccharides of human serum IgG, J. Exp. Med. 167 (1988) 1731–1736.
[38] K. Shikata, T. Yasuda, F. Takeuchi, T. Konishi, M. Nakata, T. Mizuochi, Structural changes in the oligosaccharide moiety of human IgG with aging, Glycoconj. J. 15 (1998) 683–689.
[39] E. Yamada, Y. Tsukamoto, R. Sasaki, K. Yagyu, N. Takahashi, Structural changes of immunoglobulin G oligosaccharides with age in healthy human serum, Glycoconj. J. 14 (1997) 401–405.
[40] A. Bondt, M.H. Selman, A.M. Deelder, J.M. Hazes, S.P. Willemsen, M. Wuhrer, R.J. Dolhain, Association between galactosylation of immunoglobulin G and improvement of rheumatoid arthritis during pregnancy is independent of sialylation, J. Proteome Res. 12 (2013) 4522–4531.
[41] L.R. Ruhaak, H.W. Uh, A.M. Deelder, R.E. Dolhain, M. Wuhrer, Total plasma N-glycome changes during pregnancy, J. Proteome Res. 13 (2014) 1657–1668.
[42] B. Adamczyk, T. Tharmalingam, P.M. Rudd, Glycans as cancer biomarkers, Biochim. Biophys. Acta 1820 (2012) 1347–1353.
[43] A. Almeida, D. Kolarich, The promise of protein glycosylation for personalised medicine, Biochimica et Biophysica Acta (BBA) - General Subjects.
[44] L.R. Ruhaak, S. Miyamoto, C.B. Lebrilla, Developments in the identification of glycan biomarkers for the detection of cancer, Mol. Cell. Proteomics 12 (2013) 846–855.
[45] A. Knezevic, O. Polasek, O. Gornik, I. Rudan, H. Campbell, C. Hayward, A. Wright, I. Kolcic, N. O'Donoghue, J. Bones, P.M. Rudd, G. Lauc, Variability, heritability and environmental determinants of human plasma N-glycome, J. Proteome Res. 8 (2009) 694–701.
[46] V. Borelli, V. Vanhooren, E. Lonardi, K.R. Reiding, M. Capri, C. Libert, P. Garagnani, S. Salvioli, C. Franceschi, M. Wuhrer, Plasma N-glycome signature of down syndrome, J. Proteome Res. 14 (2015) 4232–4245.
[47] V. Vanhooren, L. Desmyter, X.E. Liu, M. Cardelli, C. Franceschi, A. Federico, C. Libert, W. Laroy, S. Dewaele, R. Contreras, C. Chen, N-glycomic changes in serum proteins during human aging, Rejuvenation Res. 10 (2007) 521–531a.
[48] O. Gornik, J. Wagner, M. Pucic, A. Knezevic, I. Redzic, G. Lauc, Stability of N-glycan profiles in human plasma, Glycobiology 19 (2009) 1547–1553.
[49] D. Reusch, M. Haberger, T. Kailich, A.K. Heidenreich, M. Kampe, P. Bulau, M. Wuhrer, High-throughput glycosylation analysis of therapeutic immunoglobulin G by capillary gel electrophoresis using a DNA analyzer, mAbs 6 (2014) 185–196.
[50] C.T. Thiesler, S. Cajic, D. Hoffmann, C. Thiel, L. van Diepen, R. Hennig, M. Sgodda, R. Weissmann, U. Reichl, D. Steinemann, U. Diekmann, N.M. Huber, A. Oberbeck, T. Cantz, A.W. Kuss, C. Korner, A. Schambach, E. Rapp, F.F. Buettner, Glycomic characterization of induced pluripotent stem cells derived from a patient suffering from phosphomannomutase 2 congenital disorder of glycosylation, Mol. Cell. Proteomics (2016).
[51] D. Vanderschaeghe, E. Debruyne, H. Vlierberghe, N. Callewaert, J. Delanghe, Analysis of c-globulin mobility on routine clinical CE equipment: Exploring its molecular basis and potential clinical utility, Electrophoresis 30 (2009) 2617–2623.
[52] V. Vanhooren, S. Dewaele, C. Libert, S. Engelborghs, P.P. De Deyn, O. Toussaint, F. Debacq-Chainiaux, M. Poulain, Y. Glupczynski, C. Franceschi, K. Jaspers, I. van der Pluijm, J. Hoeijmakers, C.C. Chen, Serum N-glycan profile shift during human ageing, Exp. Gerontol. 45 (2010) 738–743.

[53] F. Dall'Olio, V. Vanhooren, C.C. Chen, P.E. Slagboom, M. Wuhrer, C. Franceschi, N-glycomic biomarkers of biological aging and longevity: a link with inflammaging, Ageing Res. Rev. 12 (2013) 685–698.
[54] R. Hennig, E. Rapp, R. Kottler, S. Cajic, M. Borowiak, U. Reichl, N-glycosylation fingerprinting of viral glycoproteins by xCGE-LIF, Methods Mol. Biol. 1331 (2015) 123–143.
[55] T.W. McDade, S. Williams, J.J. Snodgrass, What a drop can do: dried blood spots as a minimally invasive method for integrating biomarkers into population-based research, Demography 44 (2007) 899–925.
[56] R. Hennig, U. Reichl, E. Rapp, A software tool for automated high-throughput processing of CGE-LIF based glycoanalysis data, generated by a multiplexing capillary DNA sequencer, Glycoconj. J. 28 (2011) 331.
[57] R. Kottler, M. Mank, R. Hennig, B. Muller-Werner, B. Stahl, U. Reichl, E. Rapp, Development of a high-throughput glycoanalysis method for the characterization of oligosaccharides in human milk utilizing multiplexed capillary gel electrophoresis with laser-induced fluorescence detection, Electrophoresis 34 (2013) 2323–2336.
[58] A. Varki, R.D. Cummings, J.D. Esko, H.H. Freeze, P. Stanley, J.D. Marth, C.R. Bertozzi, G.W. Hart, M.E. Etzler, Symbol nomenclature for glycan representation, Proteomics 9 (2009) 5398–5399.
[59] D. Reusch, M. Haberger, M.H. Selman, P. Bulau, A.M. Deelder, M. Wuhrer, N. Engler, High-throughput work flow for IgG Fc-glycosylation analysis of biotechnological samples, Anal. Biochem. 432 (2013) 82–89.
[60] M.H. Selman, M. Hoffmann, G. Zauner, L.A. McDonnell, C.I. Balog, E. Rapp, A.M. Deelder, M. Wuhrer, MALDI-TOF-MS analysis of sialylated glycans and glycopeptides using 4-chloro-alpha-cyanocinnamic acid matrix, Proteomics 12 (2012) 1337–1348.
[61] M.H. Selman, R.J. Derks, A. Bondt, M. Palmblad, B. Schoenmaker, C.A. Koeleman, F.E. van de Geijn, R.J. Dolhain, A.M. Deelder, M. Wuhrer, Fc specific IgG glycosylation profiling by robust nano-reverse phase HPLC-MS using a sheath-flow ESI sprayer interface, J. Proteome 75 (2012) 1318–1329.
[62] M. Piagnerelli, K.Z. Boudjeltia, V. Nuyens, D. De Backer, F. Su, Z. Wang, J.L. Vincent, M. Vanhaeverbeek, Rapid alterations in transferrin sialylation during sepsis, Shock 24 (2005) 48–52.
[63] O. Gornik, G. Lauc, Glycosylation of serum proteins in inflammatory diseases, Dis. Markers 25 (2008) 267–278.
[64] C.M. Karsten, M.K. Pandey, J. Figge, R. Kilchenstein, P.R. Taylor, M. Rosas, J.U. McDonald, S.J. Orr, M. Berger, D. Petzold, V. Blanchard, A. Winkler, C. Hess, D.M. Reid, I.V. Majoul, R.T. Strait, N.L. Harris, G. Kohl, E. Wex, R. Ludwig, D. Zillikens, F. Nimmerjahn, F.D. Finkelman, G.D. Brown, M. Ehlers, J. Kohl, Anti-inflammatory activity of IgG1 mediated by Fc galactosylation and association of FcgammaRIIB and dectin-1, Nat. Med. 18 (2012) 1401–1406.
[65] R. Carrell, J. Travis, α1-Antitrypsin and the serpins: variation and countervariation, Trends Biochem. Sci. 10 (1985) 20–24.